UNIVERSITY *of* York

This is a repository copy of *High performance continuous-wave laser cavity enhanced polarimetry using RF-induced linewidth broadening*.

White Rose Research Online URL for this paper:
https://eprints.whiterose.ac.uk/id/eprint/178566/

Version: Published Version

Article:

White Rose
university consortium
Universities of Leeds, Sheffield & York

eprints@whiterose.ac.uk
https://eprints.whiterose.ac.uk/

High performance continuous-wave laser cavity enhanced polarimetry using RF-induced linewidth broadening

DANG-BAO-AN TRAN,[1,2,4] **ROBERT PEVERALL,**[1] **SARAH ROSSON,**[1] **KATHERINE M. MANFRED,**[1,3] **AND GRANT A. D. RITCHIE**[1,5]

[1]*Department of Chemistry, Physical and Theoretical Chemistry Laboratory, University of Oxford, South Parks Road, Oxford, OX1 3QZ, United Kingdom*

[2]*Permanent address: Department of Physics, Ho Chi Minh City University of Education, Ho Chi Minh City, Vietnam*

[3]*Wolfson Atmospheric Chemistry Laboratories, Department of Chemistry, University of York, YO10 5DD, UK*

[4]*an.tran@chem.ox.ac.uk*

[5]*grant.ritchie@chem.ox.ac.uk*

Abstract: We present precise optical rotation measurements of gaseous chiral samples using near-IR continuous-wave cavity-enhanced polarimetry. Optical rotation is determined by comparing cavity ring-down signals for two counter-propagating beams of orthogonal polarisation which are subject to polarisation rotation by the presence of both an optically active sample and a magneto-optic crystal. A broadband RF noise source applied to the laser drive current is used to tune the laser linewidth and optimise the polarimeter, and this noise-induced laser linewidth is quantified using self-heterodyne beat-note detection. We demonstrate the optical rotation measurement of gas phase samples of enantiomers of α-pinene and limonene with an optimum detection precision of 10 μdeg per cavity pass and an uncertainty in the specific rotation of $\sim$0.1 deg dm^{-1} (g/ml)$^{-1}$ and determine the specific rotation parameters at 730 nm, for (+)- and ($-$)-α-pinene to be 32.10 ± 0.13 and -32.21 ± 0.11 deg dm^{-1} (g/ml)$^{-1}$, respectively. Measurements of both a pure R-(+)-limonene sample and a non-racemic mixture of limonene of unknown enantiomeric excess are also presented, illustrating the utility of the technique.

1. Introduction

Chirality is crucial in many areas of science, from fundamental physics, where chiral molecules have been identified as candidates for the investigation of parity violation [1,2], to pharmacology, where two molecular enantiomers can show striking differences in cellular toxicity [3], and yet possess nominally identical physico-chemical properties. The precise analysis of chirality is essential in drug synthesis and biomolecular recognition. It is therefore not surprising that several optical techniques have been developed for determining molecular chirality. Examples include: optical rotation, electronic and vibrational circular dichroism (CD), microwave, femtosecond time-resolved CD and superchiral light spectroscopies, and ionization imaging [4–9]. Historically, optical rotation, *i.e.* the measurement of the change in polarization of a linearly polarized light beam passing through a chiral sample, is one of the most facile methods with which to ascertain the chirality of liquid-phase samples. Modern commercial polarimeters are ubiquitous and have a typical precision of $\sim$1 mdeg, mainly limited by the effect of birefringence.

Cavity-based polarimetry allows the interaction path length between the light beam and chiral sample to be increased manyfold, thus enhancing the detection of chirality, and allowing study of low(er) concentration samples. A variety of cavity ring-down polarimetry (CRDP) techniques

have been developed using both pulsed and continuous-wave (*cw*) lasers in the visible and near-IR regions [10–16]. Vaccaro *et al.* demonstrated the first pulsed CRDP, using a linear cavity complete with intra-cavity λ/4 wave-plates to amplify chiral optical rotations [10,11]. While the cavity provided an increased interaction length with the sample, this was accompanied by increased linear birefringence due to the intra-cavity optics. More recently, pulsed CRDP methods were developed by Rakitzis and co-workers using bow-tie cavities, employing two counterpropagating beams [12–15]. In this case, the effect of the intra-cavity birefringence was compensated by a signal reversing technique and a Faraday rotation offset is induced by an intra-cavity magneto-optic crystal. These devices had ring-down times, τ_0, of between 0.5 and 1 μs and were used for measuring chiral optical activity in a range of environments, including pressure-controlled vapours, open-air, and in solution. In general, pulsed CRDP utilizes lasers that are typically expensive, relatively bulky, and have large optical linewidths (> 1 GHz). Moreover, multi-exponential decays can occur because of excitation of multiple cavity modes and the resultant mode interference-induced intensity fluctuations can lead to a reduction in the sensitivity. These issues can be addressed by using *cw* lasers and recently we have reported on the development of *cw* diode laser based CRDP [16] within a bow-tie cavity for interrogating gaseous and liquid phase samples. Key to the methodology was the application of RF noise to the injection current of the diode laser to controllably broaden its linewidth and thereby ensure consistent and optimal excitation of both polarization modes.

In this paper, we present first measurements of the RF noise-induced laser broadening using self-heterodyne beat-note detection, and explicitly show that tuning the linewidth leads to an increased detection sensitivity. We also describe an augmented experimental device consisting of a low-loss intra-cavity gas cell which affords an increased baseline cavity ring-down time in excess of 9 μs. We then demonstrate the improved precision of the method by presenting optical rotation measurements of vapour of enantiomers of α-pinene and limonene at 730 nm. The optimum detection precision is determined to be 10 μdeg per cavity round trip while the specific rotation can be measured with ∼0.1 deg dm^{-1}(g/ml)$^{-1}$ uncertainty.

2. Experimental setup

An illustration of the experimental apparatus is shown in Fig. 1. After beam shaping so as to mimic the TEM$_{00}$ mode of the bow-tie cavity, the light of an external-cavity *cw* laser diode at λ_0 ∼730 nm (Sacher Lasertechnik) is directed to an acousto-optic modulator (AOM, MT80-A1-IR, AA Optio-Electronic). The resulting first diffraction beam at $\nu_0 + 80$ MHz is separated into clockwise (CW) and counter-clockwise (CCW) beams by a beam-splitter and then injected into the cavity such that they counter-propagate. The cavity is constructed from four high-reflectivity plano-concave mirrors (Layertec, radius of curvature of 1 m, diameter of 25.4 mm, and reflectivity of ∼0.9999). The cavity mirrors are separated by a distance of ∼116 cm and ∼15 cm over the long and short dimensions, yielding a total cavity length of $L = 462.3 \pm 0.4$ cm. Two Glan-Taylor polarizers (GTP) are located at the cavity inputs to filter and fix the polarization state of the beams.

A Terbium Gallium Garnet (TGG) crystal (Moltech, Verdet constant of ∼100 rad (T m)$^{-1}$ at 730 nm) is inserted in one arm of the cavity to induce a large polarization rotation ϕ_F. The TGG crystal is located within a magnetic field of B ∼0.19 T, provided by a pair of ring magnets, and results in ϕ_F∼3.3°. It has been anti-reflection (AR) coated on both surfaces with a minimum reflectivity of ∼0.05% and the empty cavity ring-down time, τ_0, is ∼11 μs. To induce cavity ring-down signals, the cavity length is swept, crossing several cavity resonances, by applying a triangle-wave signal to a piezo-electric actuator on one of the cavity mirrors. The ring-down traces are detected by two photo-multiplier tubes (Hamamatsu H10721-20). The detected signals are amplified by two transimpedance amplifiers (FEMTO, DHCPA-100) and then acquired by a high-bandwidth oscilloscope (MSO Infiniium Agilent).
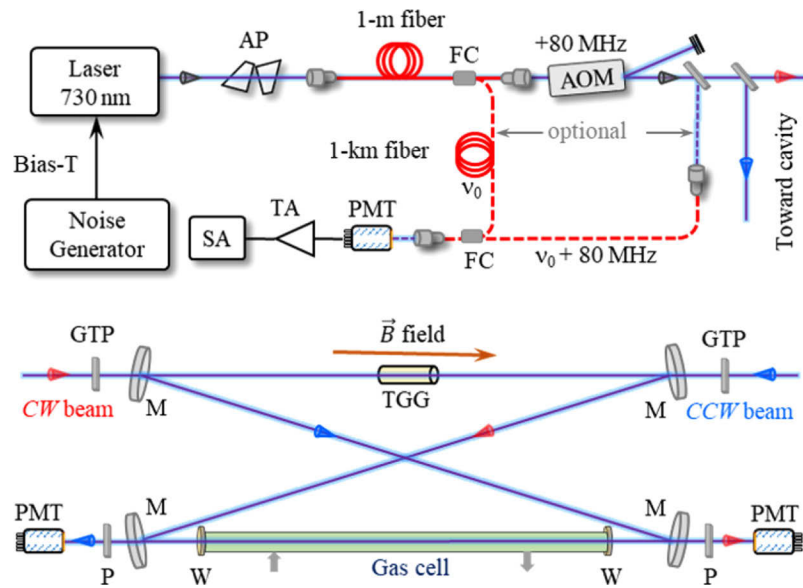
Fig. 1. Experimental setup for the continuous-wave cavity-based polarimetry at 730 nm and the measurement of the laser linewidth using self-heterodyne beat-note detection, see text for more details. Arrows of the gas cell indicate gas inlet and outlet. AP: a pair of anamorphic prisms; FC: fiber coupler; AOM: acousto-optics modulator; TA: transimpedance amplifier, SA: spectrum analyser; GTP: Glan-Taylor polariser; TGG: Terbium Gallium Garnet crystal, P: plate polariser; M: cavity mirror; W: window; and PMT: photo-multiplier tube.

Two plate polarizers (P) are placed at the cavity outputs to analyse the projection of the polarization states of the output beams and a time-dependent signal is detected, that is an exponential ring-down signal superimposed with a periodic function,

$$I(t) = A\exp\left(-\frac{t}{\tau_0}\right)\left[\cos^2(2\pi ft + \varphi) + C\right] \qquad (1)$$

where A is the amplitude of the signal, τ_0 is the ring-down time, $f = c\phi/2\pi L$ is the polarization beating frequency with ϕ the single-pass rotation angle, φ is the global phase offset, and C accounts for any reduction in the polarization-modulation depth.

A gas cell (length of 79.8 ± 0.1 cm) is inserted in one arm of the cavity for the gas-phase optical rotation measurement. It is enclosed by two 1-inch diameter, 3 mm thick, ion beam sputtered AR-coated ($R<0.02\%$) fused-silica windows (Tower Optical Corp.). The windows are placed in two home-made holders which are connected to a KF-16 tube and two KF 3-way tees (for inlet/outlet gas and pressure gauges). For each home-made holder, there are two nitrile O-rings, sticking to both surfaces of the window to minimise the effects of birefringence. The baseline cell pressure is below 10^{-5} mbar, as maintained by a turbo molecular pump (Leybold, TurboVac 360), while its working pressure was a few mbar as measured by two calibrated capacitance manometers (Ceravac CTR100 and MKS 622). Chiral samples were contained in a glass reservoir and their vapour injected into the cell via a dosing valve.

Once a chiral sample is inserted into the cell, a chiral optical rotation of ϕ_c is produced and has opposite sign for the CW and CCW beams. The oscillating frequencies of the ring-down signals relating to the polarization rotation inside the cavity are now different and given by $f_{CW} = c(\phi_F + \phi_c)/2\pi L$ and $f_{CCW} = c(\phi_F - \phi_c)/2\pi L$. The chiral optical rotation is then determined

by the following expression,

$$\phi_c = \frac{\pi L}{c}(f_{CW} - f_{CCW}).\tag{2}$$

For further details of the methodology the reader is referred to Ref. [16] which includes a detailed description from the first version of the experiment.

3. Results and discussion

3.1. Improving the sensitivity of the polarimeter

Due to the Faraday effect [17], each cavity mode is split into two circularly-polarized resonances (left and right) with a frequency separation of $\Delta f = c\phi_F/\pi L$ (~1.2 MHz with $\phi_F = 3.3°$), and which is comparable to the laser linewidth. The ring-down signal can thus be dominated by one of the two circularly polarized modes, resulting in a reduction in the modulation-polarization depth ($C > 0$) and limiting the detection sensitivity [16]. Figure 2(b) highlights this effect and shows exemplar empty cavity ring-down signals for both CW and CCW beams under conditions of a free-running laser. By fitting the model given by Eq. (1) to the data, the modulation-polarization depth is found to be C ~7 for both channels. The ring-down time is ~9 μs and corresponds to ~590 round trips inside the cavity and an effective path length through the sample cell of 0.47 km.
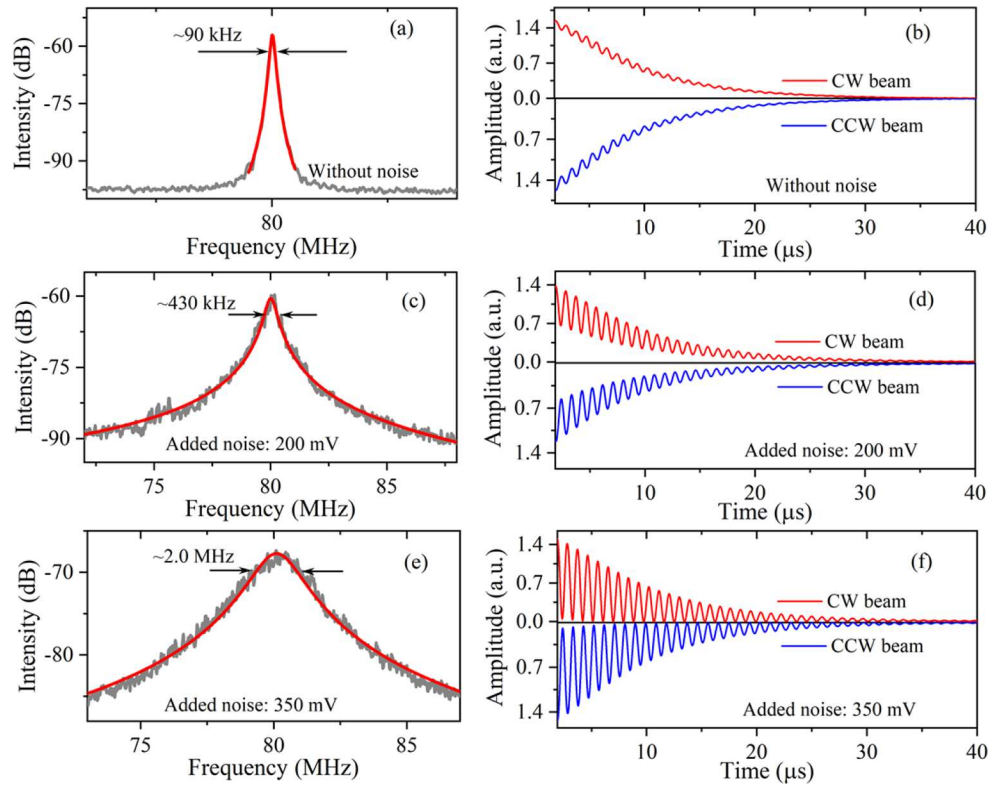

Fig. 2. Beat-note signals (gray) from the self-heterodyne linewidth measurement without (a) and with added noise of 200 mV (c) and 350 mV (e) peak-to-peak amplitude. The red curves are Lorentzian fits to the data. The associated experimental cavity ring-down signals for the CW and CCW beams under the same conditions are shown in panels (b), (d) and (f).

A robust and effective way for enhancing the sensitivity of the polarimetry is to apply a RF noise signal generated by a function/noise generator (RIGOL, DG1022) to the laser current via a bias-T input, thereby broadening the laser linewidth [16–18]. We use self-heterodyne beat-note detection to measure the laser linewidth at different added noise voltages, ranging from zero to 400 mV (Fig. 2). For this purpose, the laser beam from the 1 m short fibre is split into two branches by a fiber coupler, with the first branch directed to the AOM while the other one is injected into a 1 km long fibre which acts as a ~5 µs delay line (see Fig. 1). A fraction of the first-order diffracted free-space beam at frequency $v_0 + 80$MHz is coupled into a second fiber and combined with the output from the 1 km fiber (frequency of v_0). The output of this second fiber is detected using a photo-multiplier tube and a network/spectrum analyser (SA, HP 4895A) used to acquire the beat note signal at 80 MHz.

Figure 2(a), (c), and (e) show exemplar beat-note signals with zero-, 200- and 350-mV added-noise, which are averaged over 20 measurements and recorded at a resolution bandwidth of 30 kHz. A Lorentzian fit to the beat-note signals is normally used to determine the full-width at half-maximum linewidth (at −3 dB). The laser linewidth is then given by the resulting beat-note linewidth divided by $\sqrt{2}$ and shown in Fig. 3(a). For applied voltages of 200 mV and above, a Lorentzian lineshape fits the beat-note data very well, and the data are a good representation of the laser linewidth. As expected, the laser linewidth increases nearly linearly with a gradient of ~9 MHz/V of applied noise over the range $0.2 - 0.4$ V. We note that when the laser coherence time is larger than the optical delay, this simple model for the linewidth is no longer optimal [19]. Therefore, for applied voltages up to 150 mV we report only the apparent linewidth from a FWHM of the beat-note data, and include these data points in Fig. 3(a) for completeness while emphasising that we are predominantly interested in the linewidth regime for which the performance of the polarimeter is enhanced. We plot in Fig. 3(b) the variation of the modulation-polarization depth (factor C in Eq. (1)) as a function of the added-noise voltage. The modulation amplitude approaches unity when the added noise voltage is above 300 mV and has little effect beyond this, consistent with a cavity mode splitting of ~1.2 MHz.
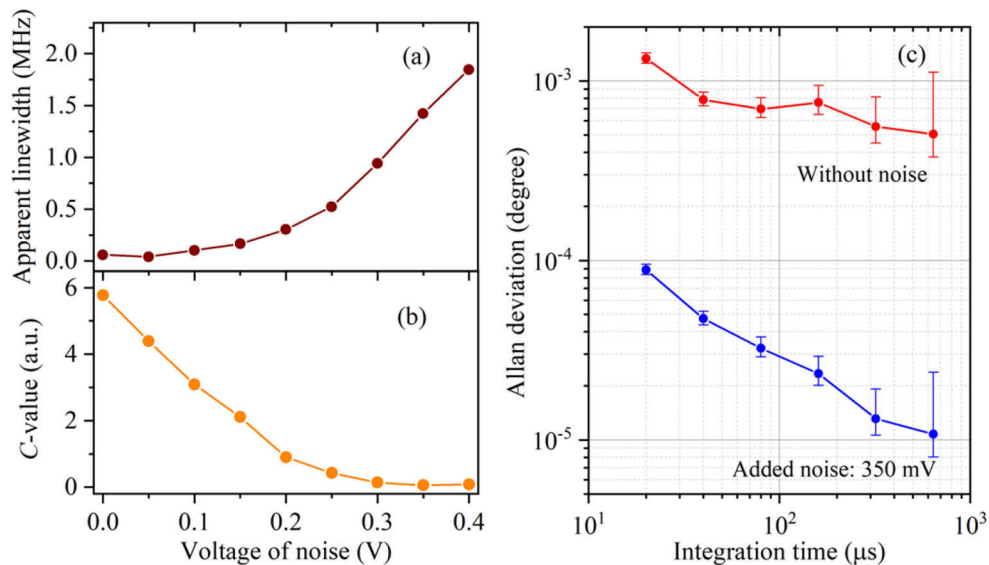

Fig. 3. Variation of the laser linewidth (FWHM) (a) and the C-value of Eq. (1) (b) as a function of the peak-to-peak voltage of the added noise. (c) Allan deviation of the chiral optical rotation with added noise (350 mV) and without.

To evaluate the stability of the polarimeter, we have measured the Allan deviation of the difference ($f_{CW} - f_{CCW}$) with no sample present and which allows the temporal characteristics of the chiral optical rotation ϕ_c to be determined. The Allan deviation, is a metric that can be used to determine the temporal stability of a measurement and ascertain optimal acquisition times, before longer term drift renders further averaging futile or even counterproductive [20]. Figure 3(c) illustrates the improvement in certainty possible in determining ϕ_c (in degrees) as a consequence of adding noise to the laser injection current. In addition, upon optimal averaging (600 s) the precision of ϕ_c improves to ~10 µdeg per cavity-pass (blue curve, Fig. 3(c)). This is at least one order of magnitude better than the case for which there is no applied RF noise (red curve, Fig. 3(c)).

3.2. Precise gas-phase optical rotation measurement on enantiomers of α-pinene and limonene

The *cw* polarimetry has been used to measure the optical rotation of gaseous (+)- and (−)-α-pinene (Sigma Aldrich, enantiomeric excess, *ee*, of *ca.* 97%) over the pressure range between 0 and 4.8 mbar. For each given pressure, we carried out tens of measurements (over a period of ~7 minutes) and determined the chiral optical rotation using Eq. (2). The uncertainty on ϕ_c of each measurement is calculated from the fitting error bars of f_{CW} and f_{CCW}. The optical rotation and its associated uncertainty at a given pressure are respectively determined by the weighted mean and 2σ weighted standard error of the corresponding 10 measurements. Note that the Faraday rotation angle, ϕ_F, is slightly different between the CW and CCW beam due to the imperfect overlapping of the laser beams and, we believe, the slight non-uniformity of the magnetic field. We thus introduce an offset frequency, δ, in Eq. (2) that can be determined easily with the empty gas cell
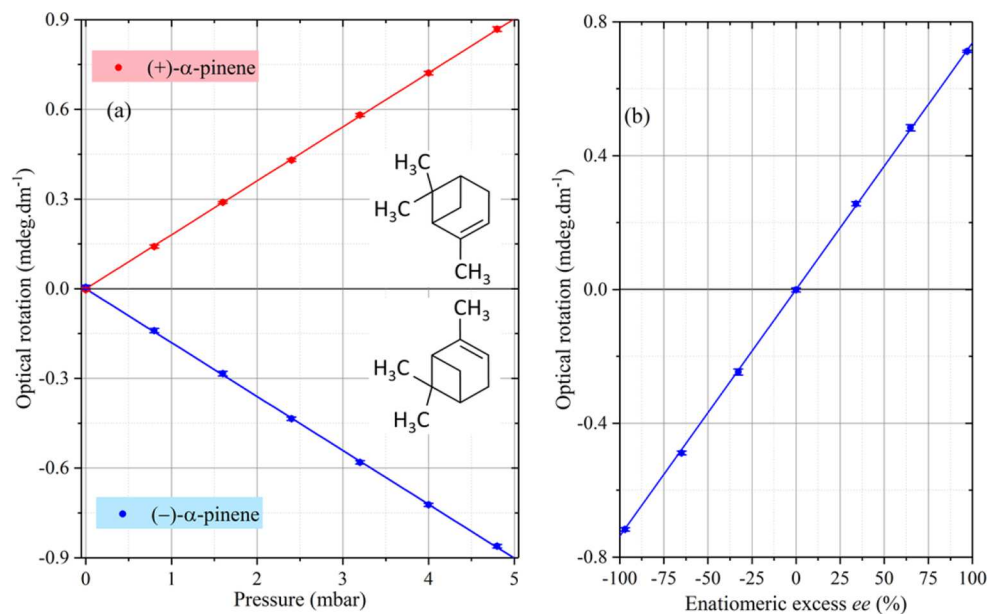

Fig. 4. (a) Gas-phase optical rotation measurement of pure (+)- and (-)-α-pinene at pressures ranging between 0 and 4.8 mbar (red and blue points, respectively). Each data point and its error are the weighted mean and 2σ weighted standard error of ten data sets at a given pressure, respectively. The red and blue lines are weighted linear fits to the data. (b) Variation of the chiral optical rotation of α-pinene mixtures with different enantiomeric excess *ee* at a fixed pressure of 4 mbar.

[16]; δ is measured to be around 7 kHz with an uncertainty below 0.02 kHz and typically does not change during the measurement. Figure 4(a) shows the variation of the chiral optical rotation as function of pressure for both pure enantiomers. During the acquisition, the pressure is stable to within ~0.01 mbar and a noise signal with a voltage of 350 mV is applied to the laser current to broaden the laser linewidth. The optical rotation precision is between 10 and 20 µdeg/pass, as determined from the error bars of ϕ_c, and is around one order of magnitude better than previous gas-phase optical rotation studies [12–14,16]. We note that this is slightly higher than the optimal precision value determined via the Allan variance (Fig. 3(c), 10 µdeg/pass), consistent with acquisition over a shorter time (400 s) than that determined for optimum performance. The red and blue lines in Fig. 4(a) are the weighted fits to the data, confirming the linear dependence between the chiral rotation and pressure. The gradient $d\phi_c/dp$ is found to be (0.1783 ± 0.0006) and (-0.1789 ± 0.0005) mdeg dm^{-1} mbar^{-1} for (+)- and (−)-α-pinene, respectively. The specific rotation parameters, $[\alpha]_{730\,\text{nm}}^{295K}$, for (+)- and (−)-$\alpha$-pinene are determined to be (32.10 ± 0.13) and (-32.21 ± 0.11) deg dm^{-1} (g/ml)$^{-1}$, respectively, where the quoted uncertainties include a contribution related to the cavity and gas-cell lengths which corresponds to ~0.07 deg dm^{-1} (g/ml)$^{-1}$. The specific optical rotation of (+)-α-pinene is in good agreement with our previous measurement of (32.4 ± 0.6) deg dm^{-1} (g/ml)$^{-1}$ [16].

We have carried out the gas-phase optical rotation measurement of α-pinene mixtures at different enantiomeric excess over the range from −97% to +97%. Two enantiomers of α-pinene are mixed at different mole fractions (assuming that the enantiomeric excess of (+)- and (−)-α-pinene is fixed at $ee = 97$ and −97%, respectively). For each given enantiomeric excess, we carried out ten chiral rotation measurement at a total pressure of 4 mbar. The measured optical rotation and its error bar are given by the weighted mean and weighted standard error of the measurements, respectively. The results are shown in Fig. 4(b). The relationship between the
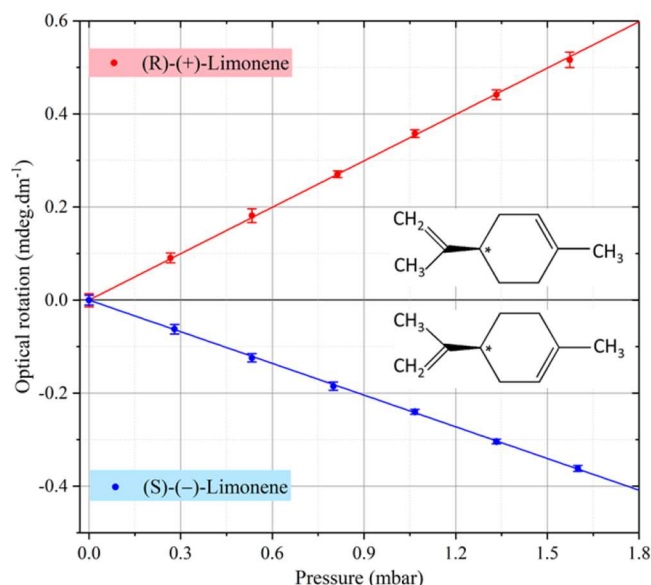

Fig. 5. Variations of optical rotation angle of (R)-(+) and (S)-(−)-limonene vapour per round-trip pass in the cavity as a function of pressure (red points and blue points, respectively). Note that the *ee* value of the (R)- sample is 99% but that for (S)-(−) is unknown. Each data point and its error are the weighted mean and 2σ weighted standard error of ten data sets at a given pressure, respectively. The red and blue lines are weighted linear fits to the data.

chiral optical rotation and *ee* is a straight line with a slope of (7.374 ± 0.0025) μdeg dm^{-1} which could be utilized for determining the enantiomer content with an unknown enantiomeric excess.

The polarimeter has also been used to perform optical rotation measurements on gaseous samples of (R)-(+)-limonene (Sigma Aldrich, *ee* = 99%) and (S)-(−)-limonene (Sigma Aldrich, unknown *ee*) at different pressures between 0 and 1.6 mbar. We follow the same procedure for measuring and analysing as in the measurement of enantiomers of α-pinene. Figure 5 (red and blue points) shows the variation of the optical rotation per unit length of (R)-(+) and (S)-(−)-limonene as a function of pressure, respectively. The red and blue lines are the weighted fits to the data with $d\phi_c/dp$= (0.3323 ± 0.0012) and (-0.2271 ± 0.0008) mdeg dm^{-1} mbar^{-1}, respectively. The specific rotation of the (nearly) enantiomerically pure (R)-(+)-limonene is found to be (59.83 ± 0.25) deg dm^{-1} (g/ml)$^{-1}$. The specific rotation of the S-(−)-limonene sample of unknown *ee* is (-40.89 ± 0.17) deg dm^{-1} (g/ml)$^{-1}$. The optical rotation of two enantiomers of a chiral molecule are identical in magnitude but of opposite sign and hence we infer that the enantiomeric excess of the commercially supplied (S)-(−)-limonene sample is ∼67%.

4. Conclusions

We have presented precise gas-phase optical rotation measurements using continuous-wave cavity-enhanced polarimetry at 730 nm. We have quantified the degree of laser linewidth broadening induced by a RF current noise and shown that it leads to improved detection sensitivity. Optimisation of the laser linewidth broadening in concert with reduced intra-cavity losses results in a polarimeter with a ring-down decay time of *ca*.10 μs and a stability of 10 μdeg per cavity pass for a 600 s integration time. The performance of the polarimeter is demonstrated by optical activity measurements of enantiomers of α-pinene and limonene with an uncertainty in the specific optical rotation of ∼0.1 deg dm^{-1} (g/ml) $^{-1}$. These improvements will allow the individual contributions to the ensemble-averaged optical rotation to be discerned.

Disclosures. The authors declare no conflicts of interest.

Data availability. Data underlying the results presented in this paper are not publicly available at this time but may be obtained from the authors upon reasonable request.

References

1. B. Darquié, C. Stoeffler, A. Shelkovnikov, C. Daussy, A. Amy-Klein, C. Chardonnet, S. Zrig, L. Guy, J. Crassous, P. Soulard, P. Asselin, T. R. Huet, P. Schwerdtfeger, R. Bast, and T. Saue, "Progress toward the first observation of parity violation in chiral molecules by high-resolution laser spectroscopy," Chirality **22**(10), 870–884 (2010).
2. A. Cournol, M. Manceau, M. Pierens, L. Lecordier, D. B. A. Tran, R. Santagata, B. Argence, A. Goncharov, O. Lopez, M. Abgrall, Y. Le Coq, R. Le Targat, H. Alvarez Martinez, W. K. Lee, D. Xu, P. E. Pottie, R. J. Hendricks, T. E. Wall, J. M. Bieniewska, B. E. Sauer, M. R. Tarbutt, A. Amy-Klein, S. K. Tokunaga, and B. Darquié, "A new experiment to test parity symmetry in cold chiral molecules using vibrational spectroscopy," Quantum Electron. **49**(3), 288–292 (2019).
3. R. Corradini, S. Sforza, T. Tedeschi, and R. Marchelli, "Chirality as a tool in nucleic acid recognition: Principles and relevance in biotechnology and in medicinal chemistry," Chirality **19**(4), 269–294 (2007).
4. P. L. Polavarapu, "Optical rotation: recent advances in determining the absolute configuration," Chirality **14**(10), 768–781 (2002).
5. N. Berova, P. L. Polavarapu, K. Nakanishi, and R. W. Woody, *Comprehensive Chiroptical Spectroscopy: Instrumentation, Methodologies, and Theoretical Simulations* (John Wiley & Sons, 2011).
6. D. Patterson, M. Schnell, and J. M. Doyle, "Enantiomer-specific detection of chiral molecules via microwave spectroscopy," Nature **497**(7450), 475–477 (2013).
7. H. Rhee, Y.-G. June, J.-S. Lee, K.-K. Lee, J.-H. Ha, Z. H. Kim, S.-J. Jeon, and M. Cho, "Femtosecond characterization of vibrational optical activity of chiral molecules," Nature **458**(7236), 310–313 (2009).
8. Y. Tang and A. E. Cohen, "Enhanced Enantioselectivity in Excitation of Chiral Molecules by Superchiral Light," Science **332**(6027), 333–336 (2011).

9. M. H. M. Janssen and I. Powis, "Detecting chirality in molecules by imaging photoelectron circular dichroism," Phys. Chem. Chem. Phys. **16**(3), 856–871 (2014).
10. T. Müller, K. B. Wiberg, and P. H. Vaccaro, "Cavity Ring-Down Polarimetry (CRDP): A New Scheme for Probing Circular Birefringence and Circular Dichroism in the Gas Phase," J. Phys. Chem. A **104**(25), 5959–5968 (2000).
11. S. M. Wilson, K. B. Wiberg, J. R. Cheeseman, M. J. Frisch, and P. H. Vaccaro, "Nonresonant Optical Activity of Isolated Organic Molecules," J. Phys. Chem. A **109**(51), 11752–11764 (2005).
12. D. Sofikitis, L. Bougas, G. E. Katsoprinakis, A. K. Spiliotis, B. Loppinet, and T. P. Rakitzis, "Evanescent-wave and ambient chiral sensing by signal-reversing cavity ringdown polarimetry," Nature **514**(7520), 76–79 (2014).
13. L. Bougas, D. Sofikitis, G. E. Katsoprinakis, A. K. Spiliotis, P. Tzallas, B. Loppinet, and T. P. Rakitzis, "Chiral cavity ring down polarimetry: Chirality and magnetometry measurements using signal reversals," J. Chem. Phys. **143**(10), 104202 (2015).
14. A. K. Spiliotis, M. Xygkis, E. Klironomou, E. Kardamaki, G. K. Boulogiannis, G. E. Katsoprinakis, D. Sofikitis, and T. P. Rakitzis, "Gas-phase optical activity measurements using a compact cavity ringdown polarimeter," Laser Phys. **30**(7), 075602 (2020).
15. A. K. Spiliotis, M. Xygkis, E. Klironomou, E. Kardamaki, G. K. Boulogiannis, G. E. Katsoprinakis, D. Sofikitis, and T. P. Rakitzis, "Optical activity of lysozyme in solution at 532 nm via signal-reversing cavity ring-down polarimetry," Chem. Phys. Lett. **747**, 137345 (2020).
16. D. B. A. Tran, K. M. Manfred, R. Peverall, and G. A. D. Ritchie, "Continuous-Wave Cavity-Enhanced Polarimetry for Optical Rotation Measurement of Chiral Molecules," Anal. Chem. **93**(13), 5403–5411 (2021).
17. L. Ciaffoni, J. Couper, G. Hancock, R. Peverall, P. A. Robbins, and G. A. D. Ritchie, "RF noise induced laser perturbation for improving the performance of non-resonant cavity enhanced absorption spectroscopy," Opt. Express **22**(14), 17030–17038 (2014).
18. K. M. Manfred, J. M. R. Kirkbride, L. Ciaffoni, R. Peverall, and G. A. D. Ritchie, "Enhancing the sensitivity of mid-IR quantum cascade laser-based cavity-enhanced absorption spectroscopy using RF current perturbation," Opt. Lett. **39**(24), 6811–6814 (2014).
19. A. Yariv and P. Yeh, *Photonics: optical electronics in modern communications* (Oxford university press, 2007).
20. E. Rubiola, *Phase noise and frequency stability in oscillators* (Cambridge University Press, 2008).